Proc. Natl. Acad. Sci. USA
Vol. 87, pp. 5682–5686, August 1990
Biophysics

Stark spectroscopy of the *Rhodobacter sphaeroides* reaction center heterodimer mutant

SHARON L. HAMMES†, LAURA MAZZOLA†, STEVEN G. BOXER†, DALE F. GAUL‡, AND CRAIG C. SCHENCK‡

*Department of Chemistry, Stanford University, Stanford, CA 94305; and ‡Department of Biochemistry, Colorado State University, Fort Collins, CO 80523

Communicated by Marshall Fixman, November 22, 1989 (received for review September 25, 1989)

ABSTRACT **The effect of an electric field has been measured on the absorption spectrum (Stark effect) of the heterodimer mutant (M)H202L of *Rhodobacter sphaeroides* reaction centers, where the primary electron donor consists of one bacteriochlorophyll *a* and one bacteriopheophytin *a*. The electronic absorption spectrum of the heterodimer mutant from 820–950 nm is relatively featureless in a poly(vinyl alcohol) film, but it exhibits some structure in a glycerol/water glass at 77 K. A feature is seen in the Stark effect spectrum of the heterodimer at 77 K centered at 927 and 936 nm in poly(vinyl alcohol) and a glycerol/water glass, respectively. This feature has approximately the same shape and width as the Stark effect for the primary electron donor of the wild type, which consists of a pair of bacteriochlorophyll *a* molecules. The angle ζ_A between the transition moment at the frequency of absorption and the difference dipole $\Delta\mu_A$ is 36 ± 2° in the wild type and 32 ± 2° for that feature in the heterodimer. A range of values for $|\Delta\mu_A| = (13–17)/f$ Debye units (where f is the local field correction) is obtained for the 936-nm feature in glycerol/water, depending on analysis method. This feature is interpreted as arising from a transition to the lower exciton state of the heterodimer, which is more strongly mixed with a low-lying charge transfer transition than in the wild type.**

With the recent availability of genes and deletion strains for the photosynthetic bacteria *Rhodobacter capsulatus* (1, 2) and *Rhodobacter sphaeroides* (3, 4), amino acid residues in the reaction center (RC) can be manipulated by site-directed mutagenesis to investigate specific aspects of protein–prosthetic group interactions. In *R. capsulatus* RCs, replacement of the histidine ligand of the M-side bacteriochlorophyll *a* (BChl*a*) molecule in the special pair primary-electron donor (denoted P) with a noncoordinating side chain leads to loss of the central Mg atom, converting it to a bacteriopheophytin *a* (BPheo*a*). This RC, the primary electron donor of which consists of one BChl*a* (D_L) and one BPheo*a* (D_M), has been called the heterodimer mutant; the symbol D is used for P in this dimer (2, 5). In contrast to P, in which the lowest singlet electronic absorption band is relatively narrow (full width at half-maximum ≈500 cm^{-1}), the absorption spectrum of D appears rather featureless and extends from ≈800–1000 nm. The quantum yield for the initial charge separation step in the heterodimer mutant is ≈50% of that in wild-type RCs; the remaining 50% of excited RCs decay rapidly to the ground state (5). The mechanism of charge separation in the heterodimer mutant has been suggested (5) to be the following:

$$DH_L \rightarrow {}^*DH_L \rightarrow (D_L^{\cdot+}D_M^{\cdot-})H_L \rightarrow (D_LD_M)^{\cdot+}H_L^{\cdot-},$$

where H_L is the BPheo*a* electron acceptor. [The notation *D is used to denote the excited state formed upon excitation at 870 nm under conditions of the experiments described in refs. 5 and 6. Internal charge transfer (CT) states of D are written as $D_L^+D_M^-$ because BPheo*a* is ≈300 meV easier to reduce than BChl*a* (5–7). The hole on D^+ may localize on the BChl*a* (D_L) half of the heterodimer.] Spectral features characteristic of the BPheo*a* anion with polarization different from that of H_L^- are present within 350 fs after excitation, which was the time resolution of the experiment (6). Thus, a significant role is postulated for intraheterodimer CT states. The possible role of CT states in determining the properties of the homodimer of the wild type—e.g., $P_L^{\cdot+}P_M^{\cdot-}$ or $P_M^{\cdot+}P_L^{\cdot-}$—has been widely discussed (8–10), but no definitive conclusion has been reached. The analogous heterodimer mutant of *R. sphaeroides* (M)H202L has now also been prepared and exhibits spectral and kinetic properties similar to those of the *R. capsulatus* mutant (C.C.S., unpublished observations).

The effect of an electric field on the absorption spectra of RCs from several different species has proven to be a useful approach for probing the dipolar character of spectroscopic transitions (11–17). The absorption Stark effect depends on the square of the magnitude of the change in dipole moment between the ground and excited states, $|\Delta\mu_A|$. When $\Delta\mu_A$ predominates over the changes in polarizability, hyperpolarizability, and the transition moment, the line shape of the Stark effect spectrum for an absorption band with a homogeneous $\Delta\mu_A$ is approximately the second derivative of its absorption spectrum (18). $|\Delta\mu_A|$ for a typical $\pi\pi$ electronic transition would be expected to be relatively small, on the order of a few Debye units, whereas $|\Delta\mu_A|$ for a CT transition will be much larger depending on the degree of CT character. Thus, the magnitude of features in the absorption Stark effect spectra of the wild-type and heterodimer mutant RCs is potentially a useful probe of the degree to which CT character is mixed into various electronic states. It is also straightforward to measure the angle ζ_A between $\Delta\mu_A$ and the transition dipole moment (12, 18). ζ_A measures the direction of charge displacement and can be related to the molecular structure when the direction of the transition dipole moment is known relative to the molecular axes. A preliminary account of these results has been presented (19).

EXPERIMENTAL METHODS

The *R. sphaeroides* heterodimer mutant (M)H202L RCs were prepared by the phosphorothioate selection method (20). Absorption Stark effects measurements were made at 77 K on samples in poly(vinyl alcohol) (PVA) films (12) and in glycerol/water glasses (21). The experimental angle χ is the angle between the electric vector of polarized light used to probe the spectrum and the electric field direction. When χ = 54.7° (the magic angle), variations in the intensity of features in the Stark spectrum due to differences in ζ_A for different bands are eliminated.

The publication costs of this article were defrayed in part by page charge payment. This article must therefore be hereby marked "*advertisement*" in accordance with 18 U.S.C. §1734 solely to indicate this fact.

Abbreviations: BChl*a*, bacteriochlorophyll *a*; BPheo*a*, bacteriopheophytin *a*; RC, reaction center; CT, charge transfer; PVA, poly(vinyl alcohol).

RESULTS

The absorption and Stark effect spectra of the wild-type and heterodimer mutant in glycerol/water glasses and the mutant in a PVA film are shown in Figs. 1–3. The most striking feature of the Stark effect spectra of the mutant is the relatively strong band at ≈930 nm (936 nm in glycerol/water, 927 nm in PVA at 77 K). Spectra are shown in both media because higher quality Stark effect data can be obtained in PVA films (the samples are free from cracks, so accurate angle measurements can be made and higher applied fields can be achieved); however, resolution is significantly better in the glycerol/water glass. This better resolution is seen most strikingly in the absorption spectrum at 1.5 K (Fig. 4*A*); a transition clearly appears at approximately the wavelength of the minimum of the lowest energy feature in the Stark effect spectrum (cf. Fig. 3*B*). ζ_A was measured for the lowest energy transition in PVA films: $\zeta_A = 32 \pm 2°$ for the heterodimer at 927 nm; $\zeta_A = 36 \pm 2°$ for the wild type at 877 nm. The entire Stark spectrum in the Q_y region was measured as a function of angle in the PVA film (data not shown). The shape of the spectra show almost no dependence on χ in the region between 820 and 1000 nm, implying that the value of ζ_A is roughly constant over this region. The intensity of the feature in the Stark effect spectrum at 927 nm in a PVA film was measured as a function of applied field between 1.5×10^5 and 4.4×10^5 V/cm and was found to be quadratic with applied field strength (data not shown); the shape of the Stark effect spectrum between 800 and 1000 nm in the PVA film was also independent of field strength.

DISCUSSION

Analysis of Data. To obtain $|\Delta\mu_A|$ from the Stark effect spectrum it is necessary to measure the second derivative of the corresponding absorption band. Obviously the curvature in the 820- to 1000-nm region of the heterodimer absorption spectrum is small, especially in PVA (Fig. 3*A*). Examination of the glycerol/water glass absorption spectrum and the Stark effect spectra in both media indicates overlapping bands in this region that differ in individual $|\Delta\mu_A|$ values. For such cases it is meaningless to simply take the second derivative

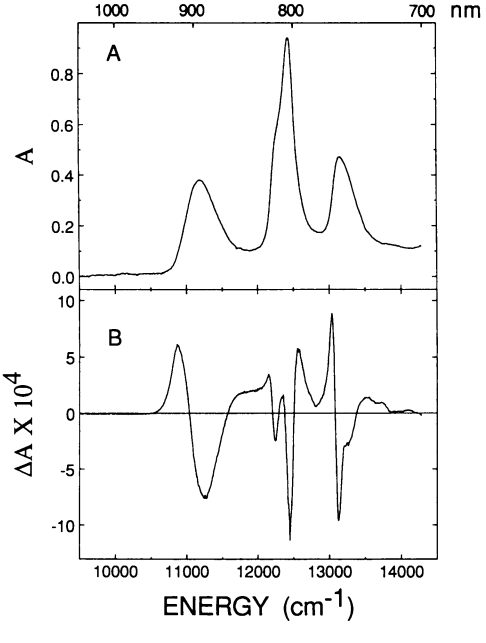

FIG. 1. Absorption (*A*) and Stark effect (*B*) spectra in the Q_y region of wild-type *R. sphaeroides* RCs at 77 K in a glycerol/water (1:1, vol/vol) glass ($F_{ext} = 2.14 \times 10^5$ V/cm, $\chi = 54.7°$).

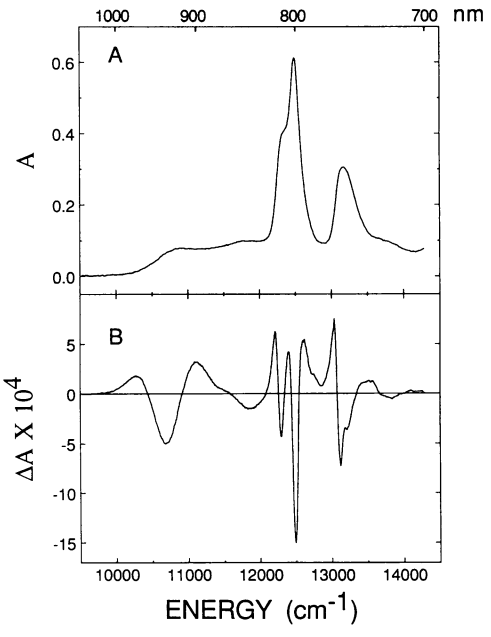

FIG. 2. Absorption (*A*) and Stark effect (*B*) spectra in the Q_y region of the heterodimer mutant (M)H202L of *R. sphaeroides* RCs at 77 K in a glycerol/water (1:1, vol/vol) glass ($F_{ext} = 2.14 \times 10^5$ V/cm, $\chi = 54.7°$).

of the overall absorption to calculate $|\Delta\mu_A|$ for underlying bands. Instead, it is essential to deconvolve the absorption spectrum into individual bands, the respective second derivatives of which can be calculated to estimate each $|\Delta\mu_A|$ separately.

The data obtained for the heterodimer mutant in the Q_y region in glycerol/water are important because there is evidence for resolved absorption features at around the same wavelengths (850 and 936 nm) as the new features in the Stark effect spectrum (see Fig. 2). For a Gaussian line shape, the separation between the zero-crossing points of the second derivative is 1.18 times smaller than the full width at half-maximum for the Gaussian.[§] An important feature of the new transition at 936 nm in the heterodimer Stark effect spectrum is that its line width, as deduced from the zero-crossing points of the Stark effect spectrum, is similar to that of the homodimer in the wild type: the zero-crossing points are separated in the wild type by 541 and 590 cm^{-1} and in the heterodimer by 476 and 681 cm^{-1} in glycerol/water and PVA, respectively (all at 77 K).

The absorption spectrum in glycerol/water was deconvolved by using the 1.5 K data (Fig. 4*A*). As a starting point, the heterodimer Stark feature at 936 nm was used to reconstruct a Gaussian band corresponding to the hypothetical heterodimer absorption in this region. The full width at half-maximum of this Gaussian band was fixed at 1.18 times the separation between the zero-crossing points of the heterodimer Stark feature, and the position of the Gaussian was fixed at the frequency of the minimum of the heterodimer Stark feature. Examination of the absorption spectrum indicates a second feature at ≈850 nm, the width of which is evidently larger than that of the 936-nm feature and which also gives rise to a much less well-defined negative feature in the Stark effect spectrum. These two components plus two components for the two resolved peaks at ≈800 nm were used

[§]The line shape is not likely to be exactly Gaussian, but this is a good approximation for the purpose of discussion. Because the Stark effect spectrum has positive and negative features, overlapping bands are especially difficult to analyze without precise line shapes for the individual underlying transitions.

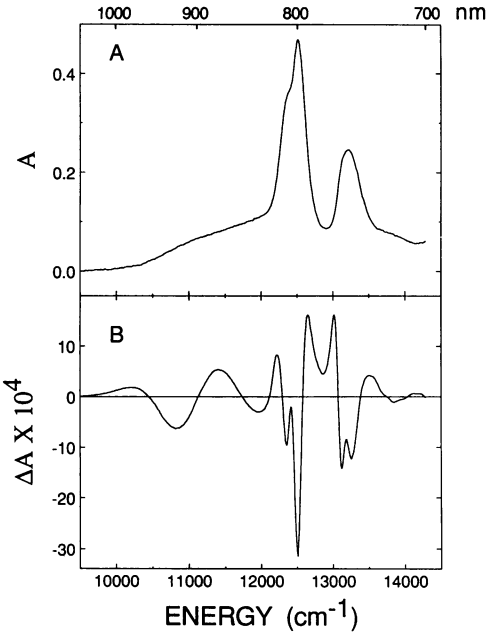

FIG. 3. Absorption (*A*) and Stark effect (*B*) spectra in the Q_y region of the heterodimer mutant (M)H202L of *R. sphaeroides* RCs at 77 K in a PVA matrix (F_{ext} = 4.98 × 10^5 V/cm, χ = 54.7°).

as a starting point to deconvolve the absorption spectrum up to the short wavelength side of the 800-nm band.§ With the width and position of the 936-nm band fixed, the best fit for the 850-nm band is approximately three times as broad as the 936-nm band (Fig. 4*B*).

$|\Delta\mu_A|$ was then calculated for the four components of the fit, neglecting possible band overlap effects. The components from the fit were scaled to the absorption spectrum of the sample used to obtain the Stark effect spectrum, and each scaled Gaussian component was used to independently find the second derivative at the maximum of the Gaussian component. ΔA was determined from the Stark effect spectrum at χ = 90° at the wavelength maximum of the Gaussian component. There is little variation in ζ_A in this wavelength region based on measurements in PVA films; the value of ζ_A used for all four components was that measured at 927 nm in PVA. The minimum value for $|\Delta\mu_A|$ of the 936-nm band is obtained by assuming that all of the absorption at 936 nm is from this band: $|\Delta\mu_A| > 13/f$ Debye units.¶

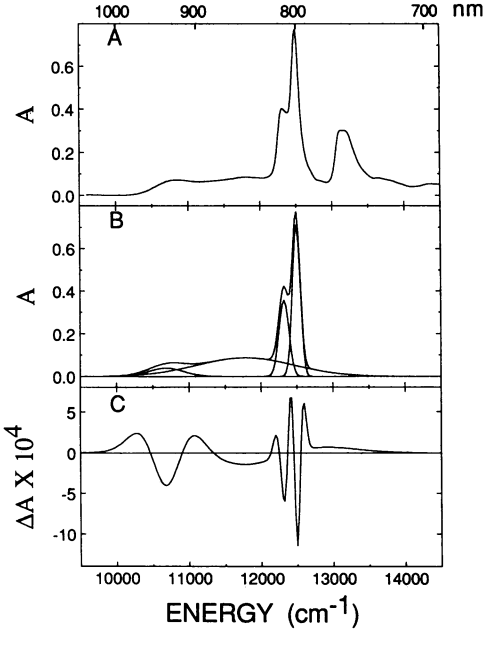

FIG. 4. (*A*) Absorption spectrum in the Q_y region of the heterodimer mutant (M)H202L of *R. sphaeroides* RCs at 1.5 K in a glycerol/water glass. (*B*) Gaussian deconvolution of the absorption spectrum in *A* as described in text. (*C*) Simulation of the Stark effect spectrum (cf. Fig. 3*B*) obtained from a sum of second derivatives of the Gaussian components from *B* weighted by $|\Delta\mu_A|^2$. Absorption maxima (cm^{-1}), full width at half-maximum (cm^{-1}), $|\Delta\mu_A|/f$ Debye units and relative amplitude for the bands are as follows: 12,497, 127, 1.5, 0.711; 12,323, 160, 1.8, 0.356; 11,787, 1582, 17.5, 0.087; 10,684, 561, 16.6, 0.039.

Even though the use of symmetric Gaussian components is undoubtedly oversimplified, it is useful to simulate the Stark effect spectrum by summing the second derivatives of each component in the deconvolution weighted by $|\Delta\mu_A|^2$ for each band. The weightings of the second derivatives of the 800 bands were varied slightly to fit the Stark spectrum better; this slight discrepancy of the weightings can be attributed to band overlap effects. The resulting simulation of the Stark effect spectrum is shown in Fig. 4*C* and agrees reasonably well with the actual spectrum (Fig. 2*B*), considering the crudeness of the model. The most serious discrepancy occurs between the 936- and 850-nm bands. When $|\Delta\mu_A|$ is calculated from the deconvolution, as described above, $|\Delta\mu_A| = 16.6/f$ Debye units for the 936-nm band, $\approx 17/f$ Debye units for the 850-nm band, and $1.5/f$ and $1.8/f$ Debye units for the monomer bacteriochlorophyll bands at 800 and 805 nm, respectively. Thus, reasonably reliable upper and lower limits are obtained for $|\Delta\mu_A|$ for the 936-nm feature, giving $|\Delta\mu_A|$ = (13-17)/*f* Debye units. Further refinement of the fitting process, such as allowing the width and the position of the 936-nm band to vary, had little effect on the derived values of $|\Delta\mu_A|$.

Although an excellent fit to the absorption spectrum between 800 and 1000 nm could be obtained using four Gaussian components, there is a persistent discrepancy in the calculated shape of the Stark effect spectrum in the region between the 850- and 936-nm bands. The line shape can be corrected, in part, by using more realistic asymmetric bands or by including small amounts of zeroth and first-derivative components in the fits, but the data do not warrant such elaborate treatments at this time. An obvious possibility to account for the peculiar line shape in the Stark effect spectrum around 900 nm is to include another, weak component. Again, although this can be done and may be warranted by considerations of the exciton components expected in this region (see below), such refinements must await further resolution of substructure by other spectral methods.

It is interesting that the absorption spectrum of the heterodimer in PVA is much less well resolved than that of the homodimer, although their Stark effect spectra are quite similar. The origin of this difference is readily understood from the width of the Stark feature in PVA compared with that in the glass. From the zero-crossing points of the red-most Stark feature, the lowest energy transition is evidently substantially broader in PVA than in glycerol/water. A similar trend is seen for the width of P in the wild type, but the difference is much smaller. The sensitivity of the heterodimer line width may result from looseness in its structure (22) when one of the anchors to the protein (the Mg–histidine bond) is removed. Making the reasonable assumption that $|\Delta\mu_A|$ for the monomer bacteriochlorophyll band at ≈800 nm is comparable in PVA and glycerol/water, the magnitudes of ΔA for the red-most Stark feature in PVA and glycerol/water can be seen to be approximately the same when corrected for

¶*f* is the local field correction: $F_{int} = f F_{ext}$, where F_{int} is the internal field experienced by the chromophores, and F_{ext} is the external applied field. The value of *f* is uncertain (probably between 1.0 and 1.5) so all values of $|\Delta\mu_A|$ are expressed as a function of *f*.

their different line widths. The implication is that $|\Delta\mu_A|$ for the feature at 936 nm in the glass sample and that for the 927-nm feature in the PVA film are comparable. An erroneously large value of $|\Delta\mu_A|$ would be obtained from analysis of the spectrum in PVA by using only the second derivative of the absorption spectrum and not considering the line width information in the Stark effect spectrum. This fact may explain why DiMagno and coworkers (23), who independently obtained absorption Stark effect data for the *R. capsulatus* heterodimer mutant in PVA, concluded that the lowest energy feature could have a very large $|\Delta\mu_A|$, suggesting a pure CT transition. We have repeated this experiment on the *R. capsulatus* heterodimer isolated from a strain generously provided by D. C. Youvan and obtain results comparable with those reported here for the *R. sphaeroides* heterodimer.

Interpretation of $|\Delta\mu_A|$ and ζ_A. To interpret the results it is necessary to combine information from several sources. At present there is no x-ray structural data for the heterodimer mutant. We will assume that the organization of the chromophores is identical to that found in the wild type (24–27). Linear dichroism data for the *R. capsulatus* heterodimer (10 K in polyacrylamide gels) suggest a relatively constant polarization to the red of the 800-nm band, the polarization being comparable to that in wild type (28). The absorption spectrum is poorly resolved under these conditions, and data were not presented for wavelengths >900 nm. The angle-dependent Stark effect data in this region exhibit a constant value of ζ_A. The value of $|\Delta\mu_A|$ for the 936-nm feature in the heterodimer [(13-17)/f Debye units] is larger than for the 870-nm feature corresponding to P in the homodimer (7/f Debye units) by about a factor of 2, and the line width of this feature is about the same as that of P. The value of ζ_A for the 936-nm band (32 ± 2°) in the heterodimer is somewhat less than that for the lowest energy 877-nm band (36 ± 2°) in the homodimer. Initially excitation of the *R. sphaeroides* heterodimer mutant at 77 K in glycerol/water at 953 nm leads to bleaching of all features at wavelengths >800 nm, suggesting that the 930-nm band and all features in the 810- to 900-nm region share a common ground state (T. Middendorf, L.M., S.G.B., and C.C.S., unpublished observations; these experiments are complicated by light-dependent spectral changes at low temperature and will be described in detail elsewhere). This result rules out the possibility that the multiple features seen in the 810- to 950-nm region result from inhomogeneous distributions of transition energies due, for example, to a looser structure in the heterodimer than in the homodimer.

Considering all this information, we suggest that the 936-nm feature in the absorption and Stark effect spectra of the heterodimer corresponds to the lower exciton component of the heterodimer—i.e., the 936-nm feature in the heterodimer is analogous to the 870-nm feature in the wild type. However, the change in dipole moment for this feature in the heterodimer is larger than that for the homodimer because the lowest-lying CT state, presumably $D_L^+D_M^-$, is considerably closer in energy to the lowest $\pi\pi$ transition, which thus acquires more CT character. The 936-nm transition is not a pure CT state because its width and $|\Delta\mu_A|$ would be expected to be substantially larger [taking the center-to-center separation of the special pair (26), a P^+P^- dipole would be ≈35 Debye units, so for $f = 1.5$,§ the observed $|\Delta\mu_A|$ would have to be ≈50/f Debye units, assuming the ground state dipole is zero]. All other things being equal one expects that the energy of a pure CT state for a heterodimer will be ≈300 meV (2400 cm^{-1}) lower than for a homodimer (5, 6) based on the lower reduction potential of BPheo*a* relative to BChl*a* (7). The oscillator strength of BPheo*a* is less than that of BChl*a*, and their Q_y transition energies in organic solvents differ by ≈300–400 cm^{-1}, so a simple exciton model predicts a smaller exciton splitting for the heterodimer than for the homodimer (all other things being equal, the exciton splitting should be reduced by at least a factor of 2). Assuming the structures are the same, the exciton contribution to the bathochromic shift for the lowest electronic transition of D should thus be smaller than that of P. Parson and Warshel (9) have stressed that mixing with CT states can profoundly affect the energy of the lowest energy exciton component in wild-type RCs. As the CT-state energy lowers, the lowest exciton band is predicted to shift to longer wavelengths. Because the $D_L^+D_M^-$ CT-state energy is certainly lower than that of P^+P^-, this model predicts that the resulting bathochromic shift of the lowest exciton component from mixing with the CT state will be even greater for D. This situation provides a rationalization for the absorption maximum of D936 relative to P870. If this rationalization is correct, then the CT state responsible for the bathochromic shift probably lies at higher energy than the lowest electronic transition that carries oscillator strength (the 936-nm band). This interpretation is inconsistent with that of refs. 5 and 6, where the initially excited *D state is suggested to evolve into a pure CT state that must have lower energy than *D. A conceivable escape from this dilemma is that mixing with even higher-lying CT states explains the red-shift. The Stark effect data presented in this paper, which suggest that the 936-nm transition has considerable CT character but is not a pure CT state, cannot distinguish between these possible interpretations.

A measurement of ζ_A for the lowest electronic transition of the RC, the functional electron-donor state, provides information on the direction of charge displacement associated with this optical transition, and a measurement of ζ_A is both very accurate and free from ambiguities concerning the local field correction (assuming f is a scalar) (12).¶ As discussed in detail elsewhere (17), for a C_2 symmetric dimer such as P, a substantial value of $|\Delta\mu_A|$ is possible; however, the direction of charge displacement must lie along the C_2 axis. Because the C_2 axis is approximately perpendicular to the transition dipole moment for P (29, 30), the observation that ζ_A is rotated to 38° implies that the electronic symmetry of ^1P is broken by some feature in its environment (17). The angle can be related to the directions of the dipoles of CT states that mix with the lowest energy transition. The angle 38° is midway between that estimated for a $P^{\cdot+}P^{\cdot-}$ and $P^{\cdot+}B^{\cdot-}$ dipole. The heterodimer, of course, does not have C_2 symmetry; however, Breton and coworkers (28) find that the transition dipole moment appears to be in approximately the same direction as for P. Thus, the observation that $\zeta_A \approx 32°$ is interesting in that it is close to the angle suggested for a state dominated by a $D_M^+D_L^-$ dipole (12), where the direction of this dipole is estimated simply as the line connecting the centers of the macrocycles using the *Rhodopseudomonas viridis* coordinates (24).

The origin of the transition or transitions in the 810- to 900-region is uncertain. The dominant band at 854 nm could originate from a CT transition. In the simulations using the minimum set of four Gaussian components, the 854-nm component has a larger line width than the 936-nm transition or P870, and the estimated value of $|\Delta\mu_A|$ is quite large. Another alternative is that the band around 854 nm is the upper exciton component of D. This state could be formulated by reducing the exciton splitting in the wild type by a factor of 2 (≈500 cm^{-1}) and by considering the difference in absorption maxima of BChl*a* and BPheo*a* in solution. In this case, rather striking variations in the linear and circular dichroism spectra in this region are expected; this result was not seen for the *R. capsulatus* heterodimer at 10 K in polyacrylamide films (28). However, as noted above, the wavelength range was somewhat limited in this study, so this region of the spectrum is being reinvestigated using a glycerol/water glass in light of the Stark effect data. The difficulties encountered in simulating the absorption and

Stark effect spectrum in the region around 850 nm suggest the presence of other transitions or vibronic structure, for which we have not yet accounted and which will be better understood after detailed low-temperature CD measurements are completed. We note, though, that evidence exists for this feature even in the Stark effect spectrum of the wild type, but it is somewhat obscured by overlap with the Q_y transition of P. There, also, a satisfactory analysis of the Stark effect line shape has not yet been obtained (17).

In conclusion, the Stark effect spectrum of the *R. sphaeroides* heterodimer mutant in the Q_y region combined with an analysis of the absorption spectrum at cryogenic temperatures in a glass indicates a transition at ≈936 nm. The oscillator strength for this transition is weaker than P870 and the change in dipole moment is larger. Furthermore, a second broader transition with a substantial difference dipole is observed at somewhat higher energy. We assign the 936-nm transition as the transition to the lower exciton state of the heterodimer that is more strongly mixed with a highly dipolar state such as $D_L^+D_M^-$ intradimer CT state than is the lower exciton state of the homodimer in the wild type. We stress that the distinction between $\pi\pi$ and CT states is a matter of degree. The approximately second-derivative line shape for the 930-nm transition, which is independent of field, implies that the field does not substantially alter the mixing between these states—i.e., they are strongly coupled (17, 31). States with substantial CT character often exhibit efficient radiationless relaxation pathways to the ground state; thus the suggestion by Kirmaier *et al.* (5) that the substantial fraction of decay to the ground state in competition with electron transfer is due to CT character appears justified. Electric field-effect spectra in other regions of the absorption spectrum and on the fluorescence are to be published elsewhere.

Note Added in Proof. A reverse heterodimer, (L)H173L, has recently been prepared. The Stark effect for the reverse heterodimer band is centered at 896 nm in a glycerol/water glass at 77K; $|\Delta\mu_A|$ is comparable to that for the 936-nm band in the (M)H202L heterodimer discussed in these pages.

We thank Drs. Breton, Holten, Kirmaier, and Norris for making data available before publication, Drs. Holten and Lockhart for very helpful discussions, and Dr. Middendorf for assistance in obtaining the 1.5 K absorption spectra. S.L.H. is a National Science Foundation Predoctoral Fellow; D.F.G. is a National Science Foundation Plant Biology Postdoctoral Fellow. Oligonucleotides were synthesized at Colorado State on equipment purchased with a National Institute of General Medical Sciences Shared Equipment Grant. This work was supported by grants from the National Science Foundation (S.G.B.), National Institutes of Health FIRST and Research Career Development Award (C.C.S.), and the Donors of the American Chemical Society Petroleum Research Fund (C.C.S.).

1. Youvan, D. C., Ismail, S. & Bylina, E. J. (1985) *Gene* **38,** 19–30.
2. Bylina, E. J. & Youvan, D. C. (1988) *Proc. Natl. Acad. Sci. USA* **85,** 7226–7230.
3. Williams, J. C., Steiner, L. A. & Feher, G. (1986) *Proteins* **1,** 312–325.
4. Gaul, D., Brasher, B., Martin, K. & Schenck, C. (1989) *Biophys. J.* **55,** 181a (abstr.).
5. Kirmaier, C., Holten, D., Bylina, E. J. & Youvan, D. C. (1988) *Proc. Natl. Acad. Sci. USA* **85,** 7562–7566.
6. Kirmaier, C., Bylina, E. J., Youvan, D. C. & Holten, D. (1989) *Chem. Phys. Letts.* **159,** 251–257.
7. Fajer, J., Brune, D. C., Davis, M. S., Forman, A. & Spaulding, L. D. (1975) *Proc. Natl. Acad. Sci. USA* **72,** 4956–4960.
8. Won, Y. & Friesner, R. A. (1988) *Biochim. Biophys. Acta* **935,** 9–18.
9. Parson, W. W. & Warshel, A. (1987) *J. Am. Chem. Soc.* **109,** 6152–6163.
10. Warshel, A., Creighton, S. & Parson, W. W. (1988) *J. Phys. Chem.* **92,** 2696–2701.
11. DeLeeuv, D., Malley, M., Butterman, G., Okamura, M. Y. & Feher, G. (1982) *Biophys. J.* **37,** 111a (abstr.).
12. Lockhart, D. J. & Boxer, S. G. (1987) *Biochemistry* **26,** 664–668, and correction (1987) **26,** 2958.
13. Boxer, S. G., Lockhart, D. J. & Middendorf, T. R. (1987) *Springer Proc. Phys.* **20,** 80–90.
14. Lockhart, D. J. & Boxer, S. G. (1988) *Proc. Natl. Acad. Sci. USA* **85,** 107–111.
15. Lösche, M., Feher, G. & Okamura, M. Y. (1987) *Proc. Natl. Acad. Sci. USA* **84,** 7537–7541.
16. Lösche, M., Feher, G. & Okamura, M. Y. (1988) in *The Photosynthetic Bacterial Reaction Center: Structure and Dynamics*, eds. Breton, J. & Vermeglio, A. (Plenum, New York), pp. 151–164.
17. Boxer, S. G., Goldstein, R. A., Lockhart, D. J., Middendorf, T. & Takiff, L. (1989) *J. Phys. Chem.* **93,** 8280–8294.
18. Liptay, W. (1974) in *Excited States*, ed. Lim, E. C. (Academic, New York), Vol. 1, pp. 129–229.
19. Boxer, S. G., Lockhart, D. J., Hammes, S., Mazzola, L., Kirmaier, C., Holten, D., Gaul, D. & Schenck, C. (1990) *Proceedings of the Eighth International Congress on Photosynthesis* (Nijhoff, Amsterdam), in press.
20. Taylor, J. W., Ott, J. & Eckstein, F. (1985) *Nucleic Acids Res.* **13,** 8764–8785.
21. Steffen, M. & Boxer, S. G. (1990) *J. Phys. Chem.*, in press.
22. Won, Y. & Friesner, R. A. (1988) *Isr. J. Chem.* **28,** 67–72.
23. Norris, J. R., DiMagno, T. J., Angerhofer, A., Chang, C.-H., El-Kabbani, O. & Schiffer, M. (1990) in *Perspectives in Photosynthesis*, eds. Jortner, J. & Pullman, B. (Kluwer, Dordrecht, F.R.G.), pp. 11–21.
24. Deisenhofer, J., Epp, O., Miki, K., Huber, R. & Michel, H. (1984) *J. Mol. Biol.* **180,** 385–398.
25. Allen, J. P., Feher, G., Yeates, T. O., Komiya, H. & Rees, D. C. (1987) *Proc. Natl. Acad. Sci. USA* **84,** 5730–5734.
26. Allen, J. P., Feher, G., Yeates, T. O., Komiya, H. & Rees, D. C. (1987) *Proc. Natl. Acad. Sci. USA* **84,** 6162–6166.
27. Chang, C. H., Tiede, D., Tang, J., Smith, U. & Norris, J. (1986) *FEBS Lett.* **205,** 82–86.
28. Breton, J., Bylina, E. J. & Youvan, D. C. (1989) *Biochemistry* **28,** 6423–6430.
29. Vermeglio, A. & Clayton, R. K. (1976) *Biochim. Biophys. Acta* **449,** 500–515.
30. Zinth, W., Sander, M., Dobler, J. & Kaiser, W. (1985) in *Springer Series in Chemical Physics on Antennas and Reaction Centers of Photosynthetic Bacteria*, ed. Michel-Beyerle, M. E. (Springer, Berlin), Vol. 42, p. 97.
31. Scherer, P. O. J. & Fischer, S. F. (1986) *Chem. Phys. Lett.* **131,** 153–159.